Adaptive Fuzzy Logic-Based Control and Management of Photovoltaic Systems with Battery Storage

Houria Assem, Toufik Azib, Farid Bouchafaa, Cherif Laarouci, Nasreddine Belhaouas, Amar Hadj Arab

Hindawi
International Transactions on Electrical Energy Systems
Volume 2023, Article ID 9065061, 18 pages
https://doi.org/10.1155/2023/9065061

Research Article

Adaptive Fuzzy Logic-Based Control and Management of Photovoltaic Systems with Battery Storage

Houria Assem,[1,2,3] **Toufik Azib**,[1] **Farid Bouchafaa**,[2] **Cherif Laarouci**,[1] **Nasreddine Belhaouas**,[3] **and Amar Hadj Arab**[3]

[1]*ESATAC'LAB, S2ET Department Ecole Supérieure des Techniques Aéronautiques et de Construction Automobile, ESTACA, 12 Rue Paul Delouvrier, Montigny-le-Bretonneux RD 10 78180, France*
[2]*Laboratoire d'Instrumentation (LINS), Faculté de Génie Electrique, Université Des Sciences et de la Technologie Houari Boumediene, USTHB, PB. 32 El-Alia, Bab Ezzouar, Algiers 16111, Algeria*
[3]*Centre de Développement des Energies Renouvelables (CDER), PB No. 62, Route de l'Observatoire 16340, Bouzareah, Algiers, Algeria*

Correspondence should be addressed to Houria Assem; h.assem@cder.dz

Received 17 January 2022; Revised 6 April 2023; Accepted 2 May 2023; Published 23 May 2023

Academic Editor: Jyotheeswara K. Reddy

Renewable energy sources (RESs) such as solar photovoltaic (PV) systems are increasingly used as distributed generation for replacing the conventional energy. At the same time, energy storage systems like battery (BAT) must be applied for maintaining the balance between fluctuating energy production and load consumption. BAT's state of charge (SOC) should be maintained within their design limits unaffected by RES intermittency and/or load power variations. This necessitates advanced power control and management methodologies for overcoming challenging conditions. This paper discusses and evaluates an optimal DC bus voltage regulation approach: an intelligent controller using an adaptive fuzzy logic controller (FLC) and a novel supervisory power management strategy for PV systems with BAT. The objectives are to keep a stable power flow in the system and guarantee the continuity of service by ensuring that the system components do not exceed their limits. In this manner, the DC bus voltage regulation of the PV/BAT system can be improved in comparison with conventional regulation. Therefore, the most important contributions of this work are as follows. (1) Development of comprehensive and modular novel energy management system (EMS): its originality is related to the inclusion of the control system limits with faster SOC balancing and smaller DC bus voltage fluctuation. (2) Providing a simple power flow management implementation that considers the optimal energy flow between PV system, BAT system, and load: a balance between minimal energy flow in the connecting line and the least requirements of BAT capacity is kept, reducing component constraints with a very straightforward structure. (3) Furthermore, FLC offers high robustness and smooth performances. FLC is added to the control strategy design requirements to reduce DC bus voltage deviation. (4) Real-time simulation/experimentation-based complete cases utilizing Matlab/Simulink and DSpace are illustrated to testify the effectiveness of the proposed FLC and EMS.

1. Introduction

1.1. Background. Recently, the demand for more accessible and eco-friendly energy has been recognized a priority issue for many countries as they attempt to reduce the greenhouse effects due to CO_2 emission from thermal power producers as well as contamination problems associated with nuclear power stations [1]. This drives representatives of over 200 countries to unite at COP24 in Katowice trying to give life to the COP21 Paris Agreement and taking into account the recent report of the GIEC 2018: to stay below +1.5°C, CO_2 emissions should be reduced by almost 50% by 2030 compared to 2010. This implies a significant transformation of the economy and industry transition. RES is emerging as an alternative means of producing clean energy [2–5]. As a result, adopting renewable energy sources (RESs) for power generation is being implemented, mainly taking advantage of solar and

wind power and installing these types of power generation systems in electrical systems [6].

Integrating the photovoltaic (PV) energy source is experiencing a sharp increase in the world [7]. It is widely developed for various applications. It is either connected to the power grid or it can participate in solving the problems of an autonomous site.

Regardless of the many benefits provided by PV energy generation, it is suffering from the unpredictability of the environment conditions and sudden changes in the power loads. To overcome this limitation, the use of an energy storage system (ESS) is required [8–11]. By utilizing a battery (BAT), a continuous power supply is provided, stabilizing the DC bus voltage and responding to load variations.

An energy management system (EMS) is necessary for this kind of systems. The EMS design is the central part of the hybrid power systems' energy distribution. It defines the coordinative task of the energy sources, ensures the maximum functionality of the system, and optimizes some important parameters (high lifetime of the system components, lower cost, higher safety coefficient, uninterrupted function, stable output, high robustness, etc.) [12].

1.2. Literature Review. Dynamic power management structures aimed at incorporating RES and ESS with DC bus have been largely exploited [13–15]. Several research papers have also focused on energy management system (EMS) in different applications of hybrid PV-BAT systems: electric vehicles, charge station, electricity, smart microgrid, etc., comparing different power management strategies and hybrid PV-BAT architectures [16–20]. Some power management approaches of hybrid PV-BAT systems for off-grid domestic households are proposed [21, 22].

In order to satisfy many objectives, researchers suggest multiple advanced control methods applied to EMSs. Various fields are implicated in developing EMSs, including linear and nonlinear algorithms [23], metaheuristic strategies [24], artificial intelligence approaches [25], stochastic programming [26], and predictive model controller [27]. Therefore, through recent research, several control strategies were proposed, involving PI/PID linear controllers, fuzzy logic controller (FLC), and artificial neural network controllers for voltage, frequency regulation, and power management [28–31]. The results show that the FLCs outperform better than the other approaches. Consequently, we will develop a similar controller for more challenging scenarios in this research. Using the FLC in hybrid RES-ESS has been intensively studied over the last few years, owing to its three most important benefits. Firstly, it is a very strong nonlinear method; secondly, it has the ability in modeling the uncertainties. Finally, no mathematical model is required as the entire system is considered as a black box [32].

For example, an EMS based on FLC in an autonomous hybrid PV-BAT-gas generator system was proposed in [33]. A water pump was used as a dump load to avoid the overcharge of the BAT. However, this method could not be applied to all power conditions. In [34], a two-stage EMS for PV-FC-BAT hybrid electric system was designed. In comparison to the conventional PI controller, this approach reduced the hydrogen consumption equivalence. In addition, the study in [35] presented an EMS that takes into account voltage stability and generation eventuality requirements. Zhang et al. [36] proposed comparative experiments with online EMS through a comparison of passive controller and finite-state machine controller approaches, highlighting the prioritization of the higher performance of the fuzzy control algorithm applied within the hybrid power system. The purpose of the EMS is to ensure that power losses, DC bus voltage fluctuations, and related costs of power generation are minimized. Furthermore, an EMS ensuring power balancing of power loads, generation sources, and battery system was suggested in [37]. The objective of the designed EMS is to try to increase the system component lifetime while seeking the highest cost-effectiveness/efficiency determined by the experts on the basis of the demand power profile. An ADVISOR-based FLC method applied to hybrid FC-BAT power was discussed, performing the power distribution between FC and BAT system, and was tested using the dSPACE hardware platform [38, 39]. Balootaki et al. [40] proposed a complete analysis of controlling and synchronizing fractional-order chaotic system switching that points out the constraints and introduced several interesting works regarding the control aspects. The suggested power system was coupling different power sources and was regarded as a highly nonlinear setup. The methodology described in [40] would be a good solution in this sense. More recently, in [41], the authors proposed an adaptive model predictive control strategy and management to regulate the voltage of local nanogrid DC bus and to provide desirable power sharing among different nanogrids without affecting their plug-and-play ability in the presence of nonlinear loads. However, BESS elements connected to the DC bus may not be able to provide good system stability due to them exceeding their power limits (current and voltage) during abrupt load variations or peak power loads as well as providing mediocre transient responses (high voltage fluctuations and ripples). In addition, these power excesses of the BESS elements can lead to their progressive degradation and thus shorten their lifetime.

1.3. Research Gap and Motivation. References mentioned above for DC-bus regulation technique and power management strategies discuss different associated techniques:

(1) Some methods are relatively sophisticated and complex that require a very high computation time. Moreover, in some cases, the required switching frequencies and sampling frequencies are also very high, which complicates the design of the converter output filters, thus making their hardware implementation much more challenging for real-time applications.

(2) Fewer studies take into consideration the dynamic response features of system units' power and endurance simultaneously. They have focused on power management aspects without constraining

some of the system's elements, such as maximum BAT power limits.

(3) In addition, in some cases, the power of the loads may vary significantly and suddenly driving the system to an unstable and nonlinear dynamic behavior. Thus, the efficient and reliable operation of the DC generator may not be ensured by linear control (e.g., PI controllers) or conventional techniques.

(4) The results of these proposed control approaches show relatively high voltage deviation on the DC link (>%2) as well as inaccurate power sharing between sources and load.

Consequently, the control of the different units (voltage/current sources) of the systems in various modes of operation under certain constraints has not yet been entirely resolved. Research on finding optimal control strategies and operating modes continues to develop.

1.4. Challenges. Typically, the challenge is to find a better trade-off between stability, performance, robustness, and reliability of the hybrid system, which addresses the following challenges:

(1) Ensure accurate power sharing and correct balancing of the BAT SOC regardless of disturbances including changing environmental conditions, power loads, and faults resulting in DC bus voltage fluctuations, overshoots or undershoots, and sags or drops [13].

(2) Consider the characteristics or limitations of the system's component units.

(3) Reduce voltage oscillations and current ripples as well as transient time.

(4) Improve the DC bus voltage regulation, which can bring better stability in the system and a clear improvement in performance. Thus, solve the above-mentioned problems related to the low dynamism of control systems with respect to the transient time of disturbances [14].

(5) Simplify the control structure and power management strategy with respect to computation time and sample rate switching, thereby making their and hardware implementations feasible and easier.

1.5. Contributions. In this regard and in order to address the above challenges, this research proposes adaptive fuzzy logic-based control and EMS for PV-BAT systems that could be applied to multiple industrial domains, namely, in DC microgrids. The innovative contributions presented in this article are as follows:

(1) A novel EMS and control structure with a comprehensive and modular system design are developed that offer flexibility for system design and improved supervisory control responsible for efficient, secure, reliable, and optimal power management and energy balancing between sources and loads. The supervisory controller adjusts the operational mode of the system components (e.g., BAT, PV, and load), and its originality is related to the inclusion of the control system limits, which presents progression with the existing approaches with respect to system conditions to achieve the system objectives.

(2) A new cascaded control loop is implemented to improve DC bus voltage regulation by using controller-based fuzzy logic with adaptive parameters, which provides high robustness and consistent performance to the system in terms of lower time transient and voltage oscillations. The FLC employs a set of fuzzy logical control rules to resolve problems related to system nonlinearities. Finally, since there is no on/off switching between the three FLCs as they work in parallel, with a progressive behavior between each other, there is no risk of instability of the system.

(3) An anti-windup compensator is added in the inner control to reduce current ripples. This anti-windup compensator only acts in the case of control value saturation. It maintains the closed-loop system in a linear domain. At this stage, the two cascaded control loops can accurately regulate the DC bus voltage while maintaining the required parameters for proper operation of the BAT.

(4) A simple implementation of power flow management (reduced component constraints with a very straightforward structure) that considers the optimal operation between the PV units, the BAT units, and the loads makes its use more advantageous.

(5) Finally, two simulation/experimentation tests utilizing Matlab/Simulink and DSpace are proposed with different scenarios to prove the continuous supply of energy when the DC bus fluctuation is below 1% even under abrupt conditions. This method brings a significant improvement with faster SOC balancing and lower DC bus voltage fluctuation (<1%) compared to the methods proposed in the literature.

1.6. Paper Organization. The rest of this article is organized as follows. Hybrid PV-BAT system description and modeling are defined in Section 2. In Section 3, the proposed adaptive FLC algorithm and power management strategy scheme are detailed. The experimental step description is described in Section 4. The results are given in Section 5, showing the effectiveness and performance of the proposed system. Finally, the conclusion summarizing the contributions of this article is reported in Section 6.

2. System Description and Modeling

2.1. System Architecture and Description. The architecture chosen for the proposed system is a parallel structure. It is the most common topology used because of its several advantages [42, 43]; indeed, the system has the advantage of being simple and relatively inexpensive, with fewer constraints on components, easy energy management, and good

reliability. In a hybrid system with a parallel structure, photovoltaic panels are considered as the primary source and storage systems as an auxiliary source coupled to the load. Referring to Figure 1, the DC bus is linked to both sources and load via static converters. Consequently, DC-DC static converters via their control devices play a key role in regulating the power from PV and BAT systems to satisfy the load requirements through the DC bus.

The system has been designed to satisfy the load requirements. A PV-BAT hybrid system is typically composed of four major components: PV system generation units; ESS based on BAT; and different loads (DC and AC). Complementary behavior is required for the primary source (PV) and its ancillary device (BAT). In addition, it is possible to calculate the system parameters to meet the load requirements. The sizing and choice of converters depend on how the PV and BAT units behave as well as on the desired load profile and application used. Consequently, the equation for maintaining the power balancing within the DC bus has to be preserved at all times:

$$\eta_{\text{Load}} P_{\text{Load}}(t) = \eta_{PV} P_{PV}(t) + \eta_{\text{BAT}} P_{\text{BAT}}(t), \tag{1}$$

where η_{pv}, η_{BAT}, and η_{Load} 906 of DC converters related to PV array, BATs, and loads, correspondingly. For the present paper, we have supposed that the power converters' efficiency average value is about 85%.

2.2. Hybrid System Modeling

2.2.1. PV Array Model. Mono-crystalline silicon PV modules are used, a single-diode PV cell model is utilized, and a series resistor is included to consider the intra-cell losses.

$$I_{PV} = I_{ph} - I_d\left[\exp\left(\frac{q(V_{PV} + R_s I_{PV})}{nkT}\right) - 1\right] - \frac{V_{PV} + R_s I_{PV}}{R_{sh}}, \tag{2}$$

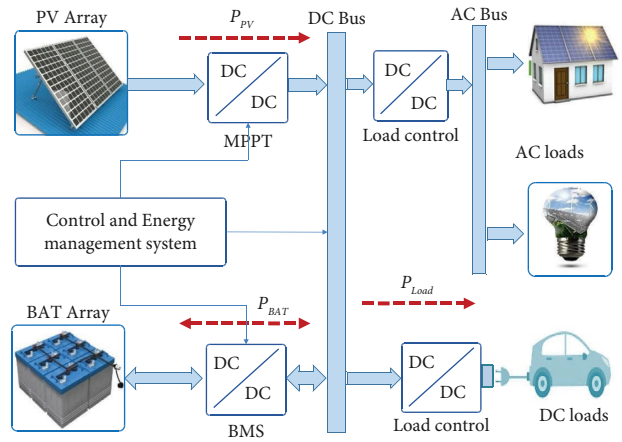

Figure 1: Typical DC microgrid parallel architecture of the PV/BAT hybrid systems.

where k represents Boltzmann's constant and T represents the PV cell surface temperature.

A PV array model can be represented by

$$\begin{cases} I_{\text{PVarray}} = N_P I_{pv}, \\ R_{\text{array}} = \dfrac{N_s}{N_P}(R_s + R_{sh}), \end{cases} \tag{3}$$

where ?$_S$ symbolizes a number of series-connected modules and ?$_P$ represent a number of parallel-connected modules.

2.2.2. Lead-Acid Battery Model. This paper used a generic model of the lead-acid BAT described in [44, 45]. The model is based on the calculation of two significant parameters representing the BAT's conduct, namely, terminal voltage, ?$_{\text{BAT}}$, and state of charge, SOC:

$$\begin{cases} V_{\text{bat}} = E_{\text{BAT}} - R_{\text{int}} I_{\text{BAT}}, \\ SOC = 100\left(1 - \dfrac{\int I_{\text{BAT}} dt}{Q_{\text{BAT}}}\right), \end{cases}$$

$$E_{\text{BAT}} = E_0 - k\frac{1 - SOC}{SOC} Q_{\text{BAT}} + A \quad \exp\{-B(1 - SOC)Q_{\text{BAT}}\},$$

$$\begin{cases} \text{Discharge: } V_{\text{BAT}}(t) = E_0 - R.I_{\text{BAT}} - K\dfrac{Q}{Q - I_{\text{BAT}} t}(I_{\text{BAT}} t + i^*) + \text{Exp}(t), \\ \text{Charge: } V_{\text{BAT}}(t) = E_0 - R.I_{\text{BAT}} - K\dfrac{Q}{I_{\text{BAT}} t - 0.1Q} i^* - K\dfrac{Q}{Q - I_{\text{BAT}} t} I_{\text{BAT}} t + \text{Exp}(t), \\ i^* = \text{filtered current } (A), \\ I_{\text{BAT}} t = \int i_{\text{BAT}} dt = \text{actual battery charge } (Ah). \end{cases} \tag{4}$$

The model includes E_0 modeling the BAT's open-circuit voltage, ?, and ?int modeling, respectively, the capacity (Ah) and internal resistance (Ω) of the BAT. K represents the polarization voltage (V/(Ah)), A is the exponential voltage (V), and B is the exponential capacity ((Ah)−1)) [45].

2.2.3. PV Boost Converter. The PV array is linked to the DC bus through a unidirectional DC/DC boost converter. The topology of the boost converter is shown in Figure 2.

By the definition of α_{pv} as the duty cycle of the converter controller, this sub-unit can be depicted by its mean model:

$$\begin{aligned} v_{\text{Bus}} &= \frac{v_{pv}}{1-\alpha_{pv}}, \\ \frac{\mathrm{d}v_{pv}}{\mathrm{d}t} &= \frac{i_{pv}-i_{Lpv}}{L_{pv}}, \\ \frac{\mathrm{d}i_{L_{pv}}}{\mathrm{d}t} &= \frac{v_{pv}-v_{\text{Bus}}\left(1-u_{pv}\right)}{L_{pv}}, \\ \frac{\mathrm{d}i_{pv}}{\mathrm{d}t} &= \frac{1}{L_{pv}}\left(-\left(1-\alpha_{pv}\right)v_{\text{Bus}}+v_{pv}\right). \end{aligned} \tag{5}$$

The voltage ripple can be calculated from equation (7).

$$L_{\min} = \frac{\alpha_{pv}\left(1-\alpha_{pv}\right)^2 R}{2f}, \tag{6}$$

where $L_{\min}$ is the inductance minimum value for continuous operation, since the inductance function is filtering the commutation frequency; α_{pv} is the duty cycle; R is the resistance of the load; and f is the commutation frequency.

$$\frac{\Delta v_{\text{Bus}}}{v_{\text{Bus}}} = \frac{\alpha_{pv}}{RCf}, \tag{7}$$

where v_{Bus} is the output voltage and C is the capacitance.

2.2.4. BAT Buck-Boost Converter. Reversible static power converter is utilized to connect the BAT unit to the DC bus, which allows BATs to be charged or discharged. As illustrated in Figure 2, they are combined with an inductance L_{BAT} and a commutating element. The current in this element is bidirectional. Two operating modes can be defined: a buck operation mode, which corresponds to the BATs absorbing power from the DC bus, and a boost operation mode corresponding to the BATs providing power to the DC bus. For our experimental setup, BATs are characterized by a constant capacitance C and negligible losses. By the definition of α_{BAT} as the duty cycle of the converter controller, the second sub-system's average model can be expressed by the following equations:

$$\begin{aligned} \frac{\mathrm{d}i_{\text{BAT}}}{\mathrm{d}t} &= \frac{1}{L_{\text{BAT}}}\left(-\left(1-\alpha_{\text{BAT}}\right)v_{\text{Bus}}\right)+v_{\text{BAT}}, \\ \frac{dv_{\text{BAT}}}{dt} &= -\frac{i_{\text{BAT}}}{C}. \end{aligned} \tag{8}$$

A bidirectional converter can be conceived simply by joining the functionalities of the boost and buck converters and swapping their diodes with switching devices, as illustrated in Figure 2. The upper switch is utilized for operating the converter like a buck converter, switching power from higher voltage side to the lower voltage side, and the down switch is used for operating the converter like a boost converter, which transfers power from the lower voltage side to the higher voltage side.

2.3. System Operation. BAT can generally function in either charge mode or discharge mode, depending on the state of power availability-requirement between the PV and load [44]. The prolonged power unbalancing in the PV-BAT system may allow BAT deep discharging or overcharging. To extend the lifetime of BAT and fully utilize the PV power generation, the operating modes of the PV-BAT system can be divided into two modes: the operation with normal charging/discharging of BAT (normal mode) and operation with full charge/discharge of BAT (transient mode).

2.3.1. Normal Mode

(1) Charge mode: PV power output is higher than the power load requirement and $\text{SOC} < \text{SOC}_{\max}$. The surplus of power from PV is accumulated in BAT through the bidirectional converter, which will operate in this case in charge mode. The PV can function in MPPT mode in order to use the RES properly as

$$P_{\text{BAT}} = P_{PV} - P_{\text{Load}}. \tag{9}$$

(2) Discharge mode: The PV power generation cannot satisfy the load consumption, and since the $\text{SOC} > \text{SOC}_{\min}$, BAT can, therefore, provide energy. The bidirectional converter operates in discharge mode for compensating the deficit power in the DC bus as follows:

$$P_{\text{Load}} = P_{PV} + P_{\text{BAT}}. \tag{10}$$

2.3.2. Transient Mode

(1) Upper limit: The PV power generation is still greater than the power load demand, and BAT is close to $\text{SOC}_{\max}$. The BAT controller intervenes for preventing the BAT overcharging, and the PV system has to quit the MPPT operating mode [46] and switch to the DC bus voltage regulation operation as

$$P_{PV} \approx P_{\text{Load}}. \tag{11}$$

(2) Lower limit: The PV power is still insufficient to satisfy the demand of the load demand, and BAT nears $\text{SOC}_{\min}$. The BAT controller intervenes to avoid the BAT deep discharging, and the low-priority load can be disconnected to preserve power balance and DC bus stability as

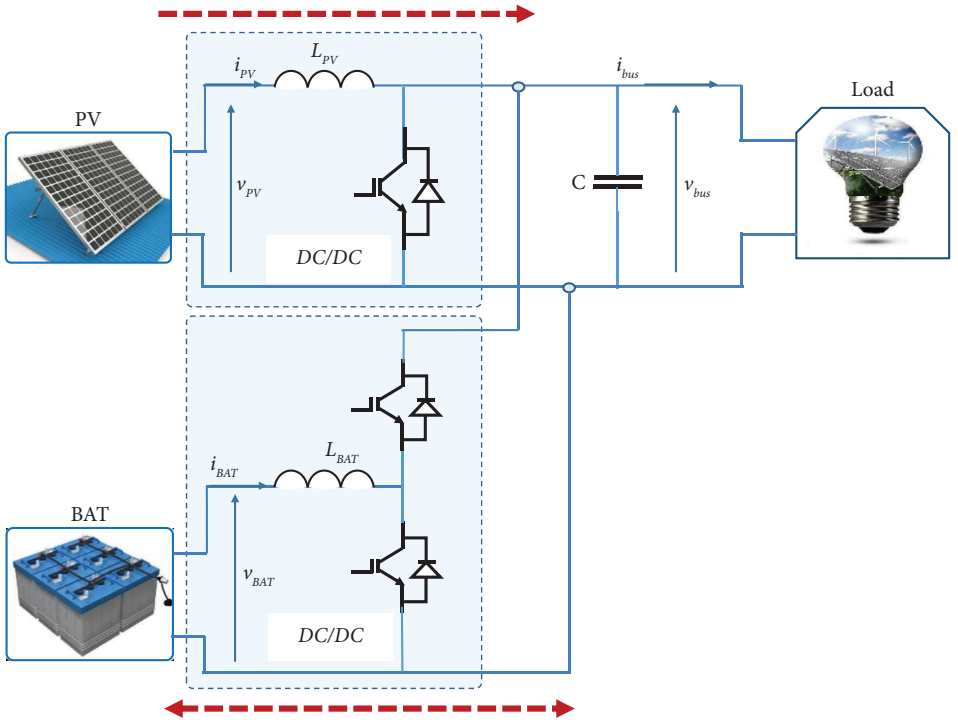

Figure 2: PV boost converter and BAT buck-boost converter model.

$$P_{\text{Load}} \approx P_{PV}. \tag{12}$$

Recharging/discharging of the BAT stops when they are fully charged/discharged.

3. Fuzzy Logic Controller and Energy Management System

The global structure of the proposed control strategy and EMS is illustrated in Figure 3 based on the cascade control loops and multi-stage power exchanging control.

In Figure 3, the main circuit scheme is shown on the top, the block diagrams of the inner current control loops are shown in the middle, and the block diagram of the multi-stage power exchanging control is shown at the bottom.

The control strategy consists of MPPT and adaptive FLC control for PV, BMS based on adaptive FLC for BAT, and voltage regulation for DC bus. These control techniques are designed to achieve the power exchange control in EMS and maintain the power balance and thus realize coordinated functioning between different units in the PV-BAT system.

3.1. Control Strategy for PV. When the PV-BAT system is operating in normal mode, i.e., BAT assumes the responsibility of the voltage balance in the DC bus, the MPPT controller controls the PV system. The MPPT technique chosen in this paper is the one using the FLC algorithm because of the benefits that it offers. The MPPT techniques performed in the authors' previous work and are reported in [47]. In transient mode, when BAT'SOC nears its maximum limit and PV generation power is high enough for the load requirement, the PV system has to take over the DC bus voltage regulation mission. Consequently, the MPPT controller will switch to the adaptive fuzzy controller for stabilizing the DC bus voltage. The structure control strategy is described in detail in Figure 4, where the switching command signal between MPPT and the fuzzy controller is derived from the EMS.

The general structure of a fuzzy logic control consists of three blocks, as shown in Figure 5: fuzzifier block, inference rule block, and finally the defuzzifier block. The membership function value is assigned to the linguistic variables by means of five fuzzy sub-sets.

The fuzzy controller consists of a fuzzy inference system (FIS) and an integrator. The adjustment of the PV reference voltage is performed following the DC bus voltage error $E(k)$. The DC bus voltage reference $V_{\text{BUS\_ref}}(k)$ is adjusted based on the inference and the fuzzy incremental output (ΔV). The membership functions (MF) are presented in Table 1 according to a set of fuzzy inference rules, as shown in Figure 6.

3.2. Control Strategy for Battery. When the PV-BAT system operates in normal mode, the BAT system is controlled by BMS. In transient mode, when SOC'BAT approaches its limitations (lower and upper limits), the reference voltage of the DC bus is compensated to correct value through the FLC block to reduce the deviations of the DC bus voltage. The detailed structure control is shown in Figure 7, and the switch choice between BMS and FLC is obtained from the EMS.

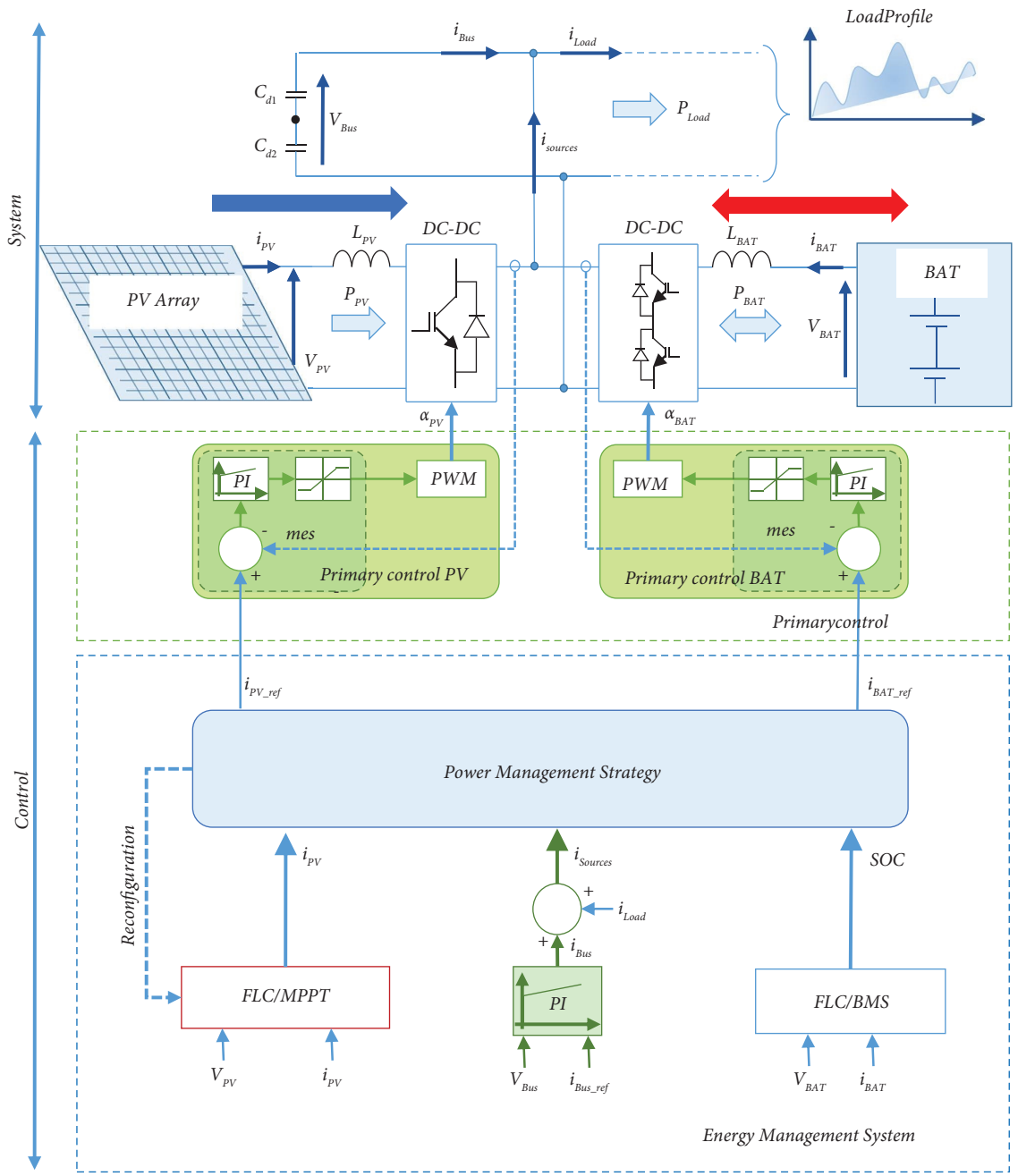

Figure 3: Proposed EMS and control and supervision design and configuration.

The proposed fuzzy battery controller (FLC-BAT) is illustrated in Figure 8. The input and output parameters of the FLC-BAT consist of two sub-systems (upper and lower) corresponding to the charging and discharging mode of the BAT, respectively.

The upper FLC-BAT sub-system is assigned to prevent the BAT from overcharging and exceeding its power-charging limit. The inputs of this sub-system are given by

$$\Delta SOC_1 = \frac{SOC^*_{\max} - SOC}{SOC^*_{\max} - SOC^*_{\min}},$$
$$\Delta P_{\text{charge}} = \frac{P^*_{\text{charge\_max}} - P_{\text{charge}}}{P^*_{\text{charge\_max}}}. \quad (13)$$

The output is a negative BAT current $i_{\text{BAT\_max}}$.

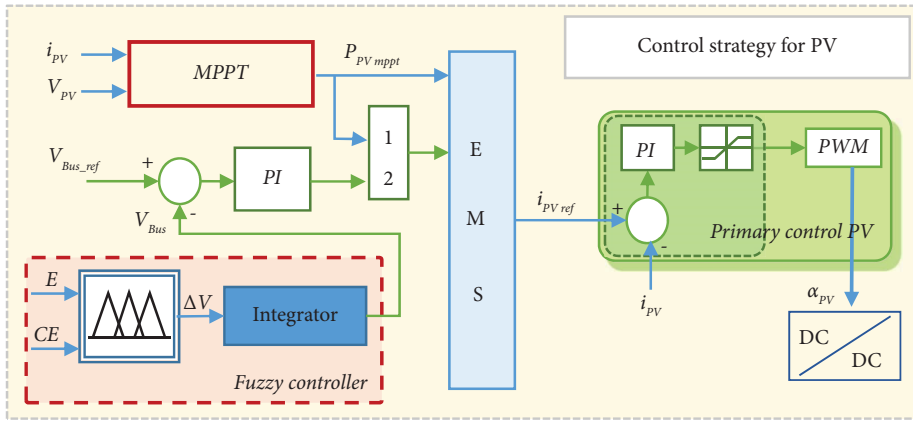

Figure 4: Structure of the PV fuzzy controller.

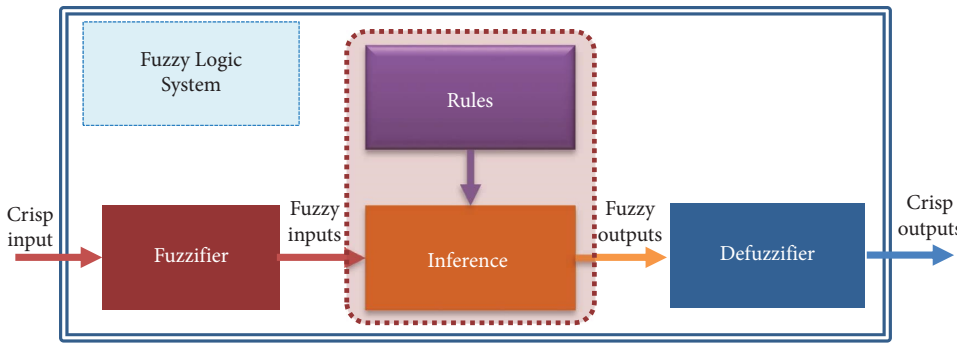

Figure 5: General structure of the fuzzy logic controller.

Table 1: Fuzzy rule table.

The input of FIS	NL	NM	NS	RZ	PS	PM	NL
The output of FIS	PL	PL	PS	RZ	NS	NL	NL

The input and output variables are symbolized as PL (positive large), PM (positive medium), PS (positive small), NL (negative large), NM (negative medium), NS (negative small), and RZ (symbolizing zero).

The lower FLC-BAT sub-system is assigned to prevent the BAT from deep discharging and exceeding its power-discharging limit. The inputs for this sub-system are given by

$$\Delta SOC_2 = \frac{SOC - SOC^*_{\min}}{SOC^*_{\min+10\%} - SOC^*_{\min}},$$
$$\Delta P_{\text{discharge}} = \frac{P^*_{\text{discharge\_max}} - P_{\text{discharge}}}{P^*_{\text{discharge\_max}}}, \quad (14)$$

where $SOC^*_{\min}$ is the SOC minimum value and $SOC^*_{\min+10\%}$ is the SOC minimum value plus 10%.

The output is a positive BAT current $i_{\text{BAT\_min}}$.

As the proposed FLC-BAT system is implemented in the EMS and depends on the bus voltage, the BAT currents will be deviated to a new $i_{\text{BAT\_ref}}$. Consequently, the PV power can also be reduced accordingly. The rules are modified in conjunction with changes in MF to evaluate the PV-BAT hybrid system's performance; therefore, modifications are made as required. More details will be given in the next section.

3.3. Energy Management Strategy. The power management system must be in a position to manage power sources: PV and BAT, to satisfy load demand and ensure that the whole system operates with high efficiency and high reliability.

The basic principle of the suggested control approach of the EMS system presented in Figure 3 is centered on smart power management supervision with cascade control loops:

(1) Primary control: The local control strategy consists of associating a current closed-loop controller to each PV and BAT source. The control is carried out using a classical PI controller through corresponding static converters: unidirectional for PV and bi-directional for BAT.

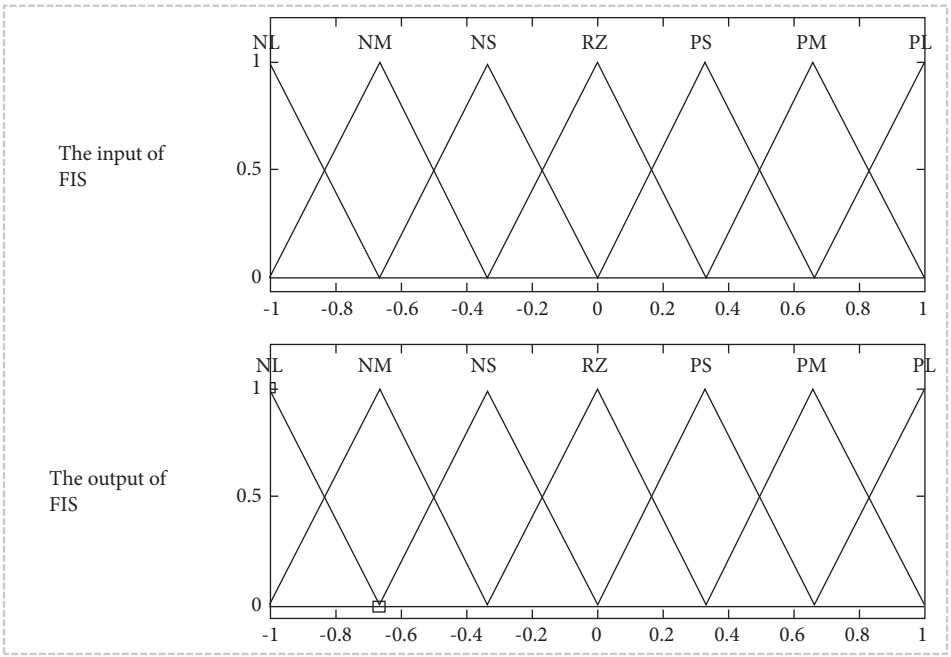

Figure 6: The membership functions of the fuzzy control.

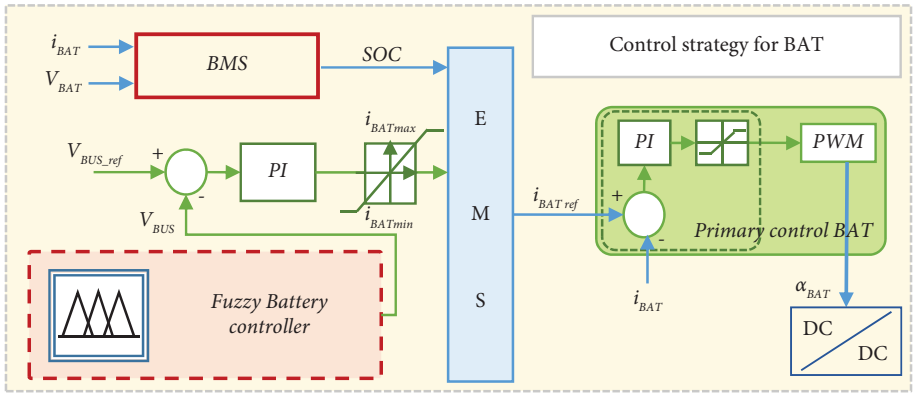

Figure 7: Structure of the fuzzy battery controller.

(2) Energy management system: The power management protocol consists in dispatching the energy provided by the PV and BAT sources with the load respecting the local control system—FLC-PV for the primary PV source and the FLC-BAT charge/discharge regulator for the auxiliary BAT source. The control strategy is based on reference currents i_{PVref} and i_{BATref} defined by the EMS corresponding to PV and BAT sources, respectively.

In a more detailed way, the operation of the management module is explained in Figure 9. The exchange of power between the sources and the load necessarily results in a modification in the DC bus voltage. Consequently, their measurements are essential in estimating the power needed by the power system supervisor.

$$\begin{cases} C_{\mathrm{Bus}}\dfrac{dv_{\mathrm{BUS}}}{dt} = i_{\mathrm{Cbus}} = i_{\mathrm{Sources}} - i_{\mathrm{Load}} \\ i_{\mathrm{Sources}} = i_{PV}^{*} + i_{BAT}^{*} = G_1 \bullet i_{PV} + G_2 \bullet i_{\mathrm{BAT}}, \end{cases} \tag{15}$$

$$G_1 = \frac{v_{\mathrm{BUS}}}{v_{PV}},$$

$$G_2 = \frac{v_{\mathrm{BUS}}}{v_{\mathrm{BAT}}}.$$

The voltage control loop has to maintain $V_{\mathrm{BUS}}\,(t)$ on its reference value, eliminate the DC bus voltage deviation, and accordingly deliver the current of sources ($i_{\mathrm{Sources}}\,(t)$).

The proposed power management system must still be integrated once the required energy sources have been identified. A k_R weighting coefficient can be used to

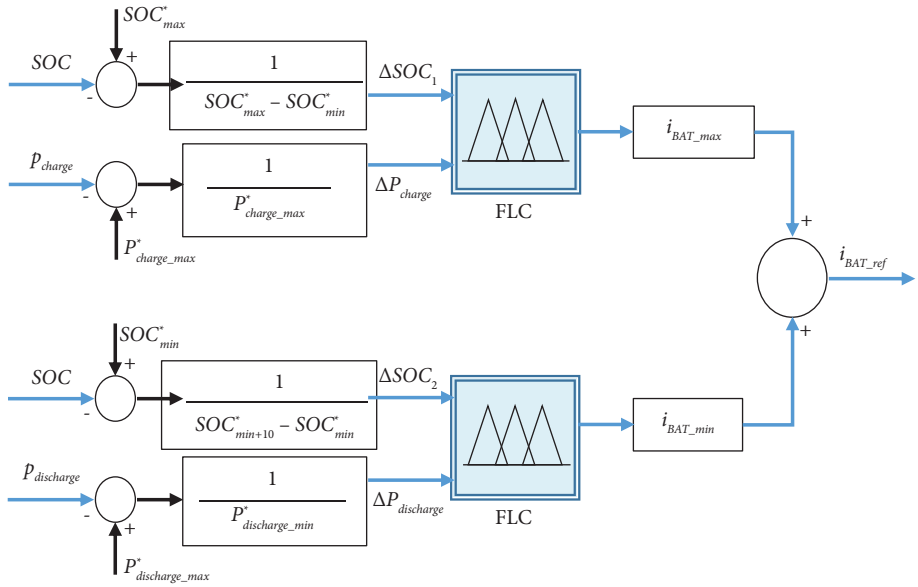

Figure 8: Structure of the fuzzy battery controller.

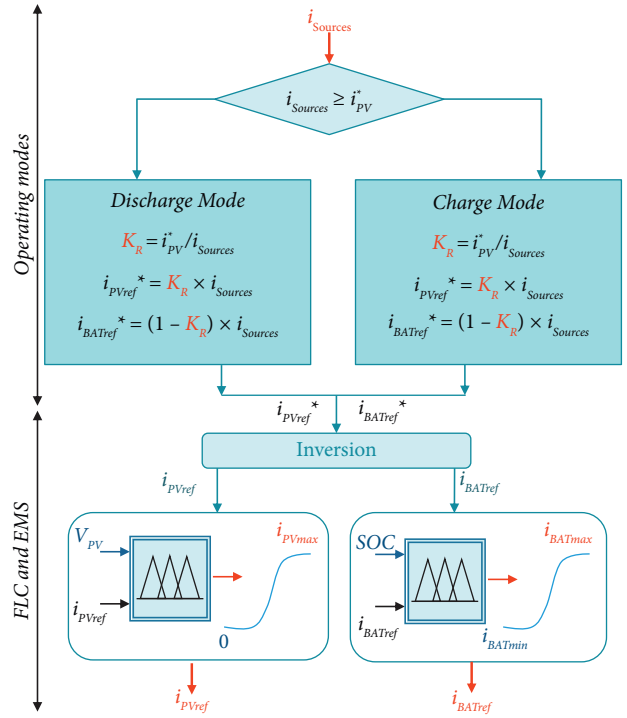

Figure 9: Control and EMS flowchart for hybrid PV-BAT hybrid systems.

implement this strategy to manage the distribution of power between PV and BAT according to the operating modes shown in Figure 9.

$$\begin{cases} i_{PV}^{*} = k_R \bullet i_{\text{Sources}}, \\ i_{\text{BAT}}^{*} = (1 - k_R) \bullet i_{\text{Sources}}. \end{cases} \tag{16}$$

It is noteworthy that the voltage and current of the BATs are limited, as well as the PV current as follows:

$$-V_{\text{BAT\_min}} \le V_{\text{BAT\_ref}} \le +V_{\text{BAT\_max}},$$
$$\begin{cases} 0 \le i_{PV} \le i_{\text{PVmax}}, \\ i_{\text{BATmin}} \le i_{\text{BAT}} \le i_{\text{BATmax}}. \end{cases} \tag{17}$$

The goal of the controller algorithm and energy management strategy is to control the converters so that they operate in appropriate modes. According to the status of PV and BAT units, the system's boundaries are to be taken into account by maintaining the SOC at the nominal values [SOC_{Min}, SOC_{Max}]. The value of the DC bus voltage is imposed by the BATs. By making this choice, the BATs have a double role: they perform their usual storage function but also allow the regulation of the DC bus voltage. On the other hand, they impose a current control strategy on the converters. The BATs provide energy stored and make sure the system works efficiently and has a good dynamic performance by recovering excess PV production.

4. Experimental Setup Description

The proposed control and EMS systems have been first built through Matlab/Simulink, as shown in Figure 10, consisting of PV and BAT systems with their DC-DC power converter. Also, the DC bus and load with control systems are used in each unit.

Closed-loop digital and physical experimentation has the potential of overcoming the restrictions of simulation and has more authenticity. To verify the proposed control strategy and EMS practically, a small-scale experimental platform (Figure11) was built up in ESTACA'LAB and the S2ET Department of the "Ecole Supérieure des Techniques

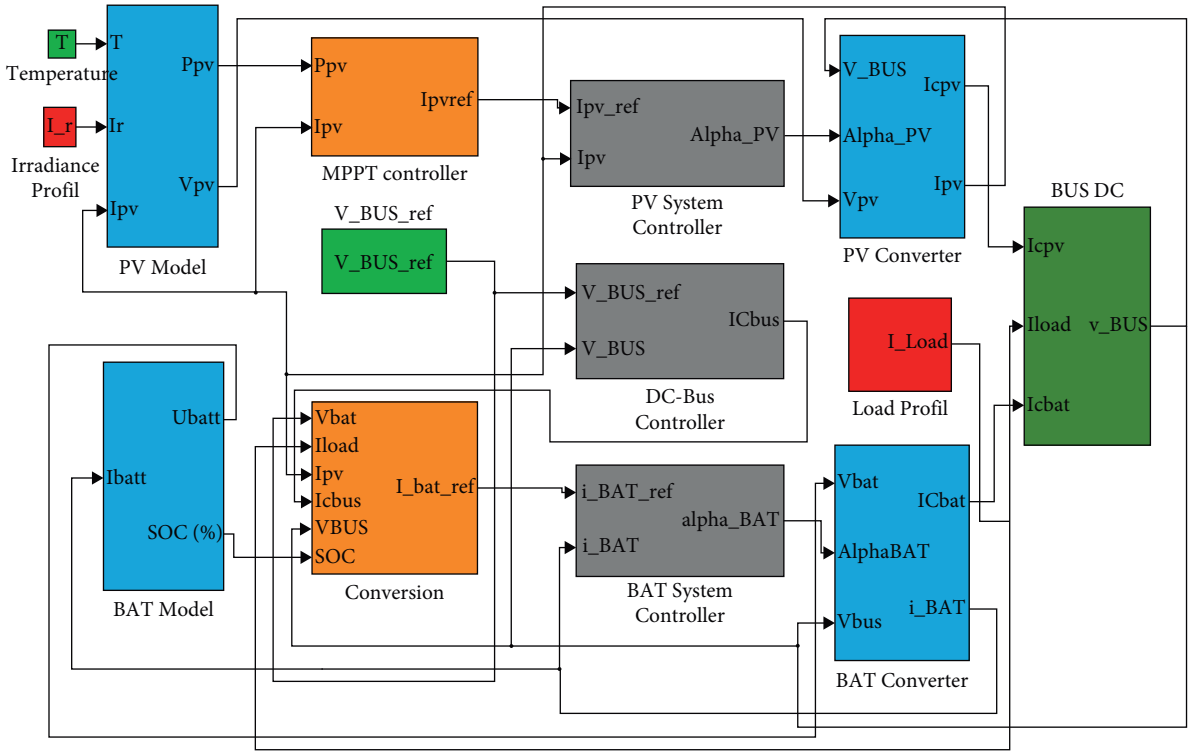

Figure 10: Graphical block of the Matlab/Simulink model used in experimental tests.

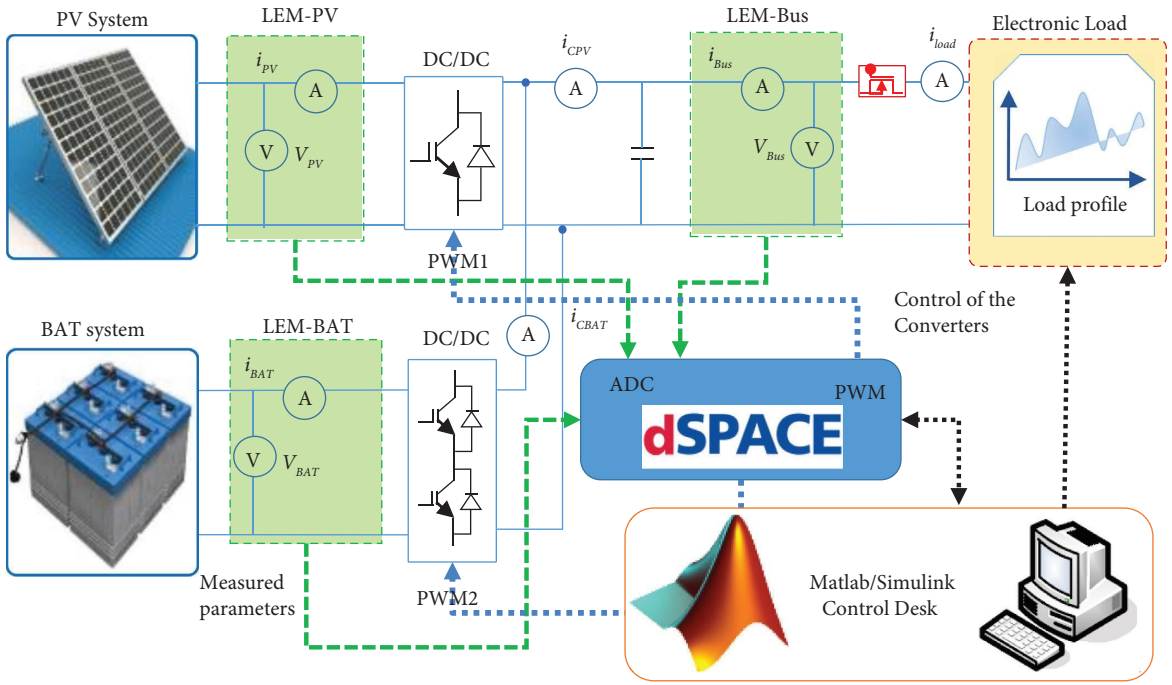

Figure 11: Structure diagram of the setup of the experimental tests.

Aéronautiques et de Construction Automobile, ESTACA" (Paris, France).

The structure diagram of the experimental test setup is shown in Figure 12. The measurement, control, and transfer signals are identified by green, blue, and black colors, respectively. As the number of supervised waveforms was huge for a complete display, signals were observed in DSpace/ControlDesk.

From Figure 11, the PV and BAT units are connected to a ZS1806 programmable electronic load with variable power

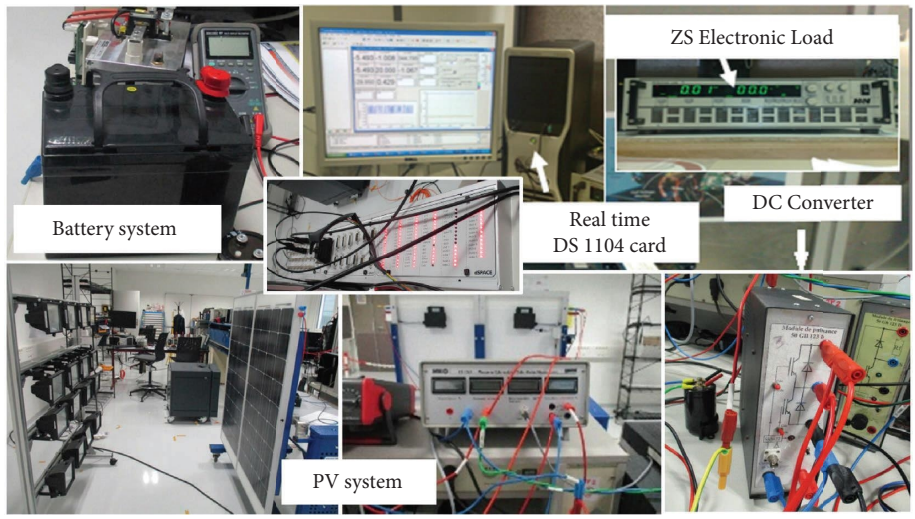

Figure 12: The constituents of the experimental tests.

Table 2: Electric characteristics of the system.

	Value
PV: parameter name	
Open-circuit voltage	44 V
Rated voltage (standard conditions)	32 V
Rated current (standard conditions)	15 A
Battery: parameter name	
Open-circuit voltage	42 V
Rated current	15 A
Internal resistance R_{int}	0.2 Ω
SOC_{min}	50%
SOC_{max}	90%
i_{BATmax}	10 A
*Inductors and*capacities*: parameter name*	
Inductors L_{PV}/L_{BAT}	100 μH
Rated currents L_{PV}/L_{BAT}	25 A
Capacities C_{BUS}	4 mF
Optimal DC-bus voltage V_{BUSref}	50 V

up to 1800 W ([0–150 A]/[0–60 V]). The measurements are transmitted to the control system via A/D converters of the DSpace control board with a sampling rate of 25 kHz, which means that the controllers provide the updated control setpoints every 50 μs. For the measurement of current and voltage, the Hall effect transducers LEM LA55-P and LV20-P were used, respectively. A DS1104 DSpace board is used to real-time test the proposed control and power management system developed and implemented in Matlab/Simulink. Additional system specifications of the relevant experimental parameters are given in Table 2 [48].

5. Results and Discussion

Two series of tests are carried out to validate the efficiency of the proposed control algorithm and EMS. In the first test, under constant solar irradiance, the control strategy is applied in normal mode, including the switching between charging and discharging modes and vice versa. The results are shown in Figure 13.

The second set of experiments, conducted under variable solar irradiance (Figure 14), allows validating the transient mode. Additionally, the results of these two series of tests (normal mode and transient mode) are compared and discussed with other authors to fully validate the efficiency of the suggested control method and EMS.

5.1. Case 1: Constant Solar Irradiance. From the results of the first tests shown in Figure 13, the power of PV and BAT sources is automatically shared through the local converters with current adjusting following the variation of power load.

Figure 13(a) shows the power on PV array, BAT, and load, respectively. The BAT provides the complementary power to ensure supply and demand balance, as shown in Figure 13(a).

Figure 13(b) shows the incidence irradiance in the PV system. The PV power varies in accordance with the solar irradiance profile. In Figure 13(b), it is clearly seen that the curve of maximum PV power tracks perfectly the curve of solar irradiance variation, despite the fluctuation of load requirements, which approves the suggested MPPT technique.

The variation of SOC in BAT is within the maximum and minimum ranges in system operation, as shown in Figure 13(f).

Figure 13(d) shows the controlled current on the PV unit and its reference provided by the MPPT algorithm. Since the irradiance curve has an influence on the current, their variations are very similar. The PV current output is maximal and constant (working under its MPP) because solar irradiance is supposed to be constant during this first series of tests.

Figure 13(e) shows the supervised current on the BAT unit and its reference provided by the second layer controller. The latter will change its path (sign) from charging mode to discharging mode at 8 h 21 to assist the PV source in

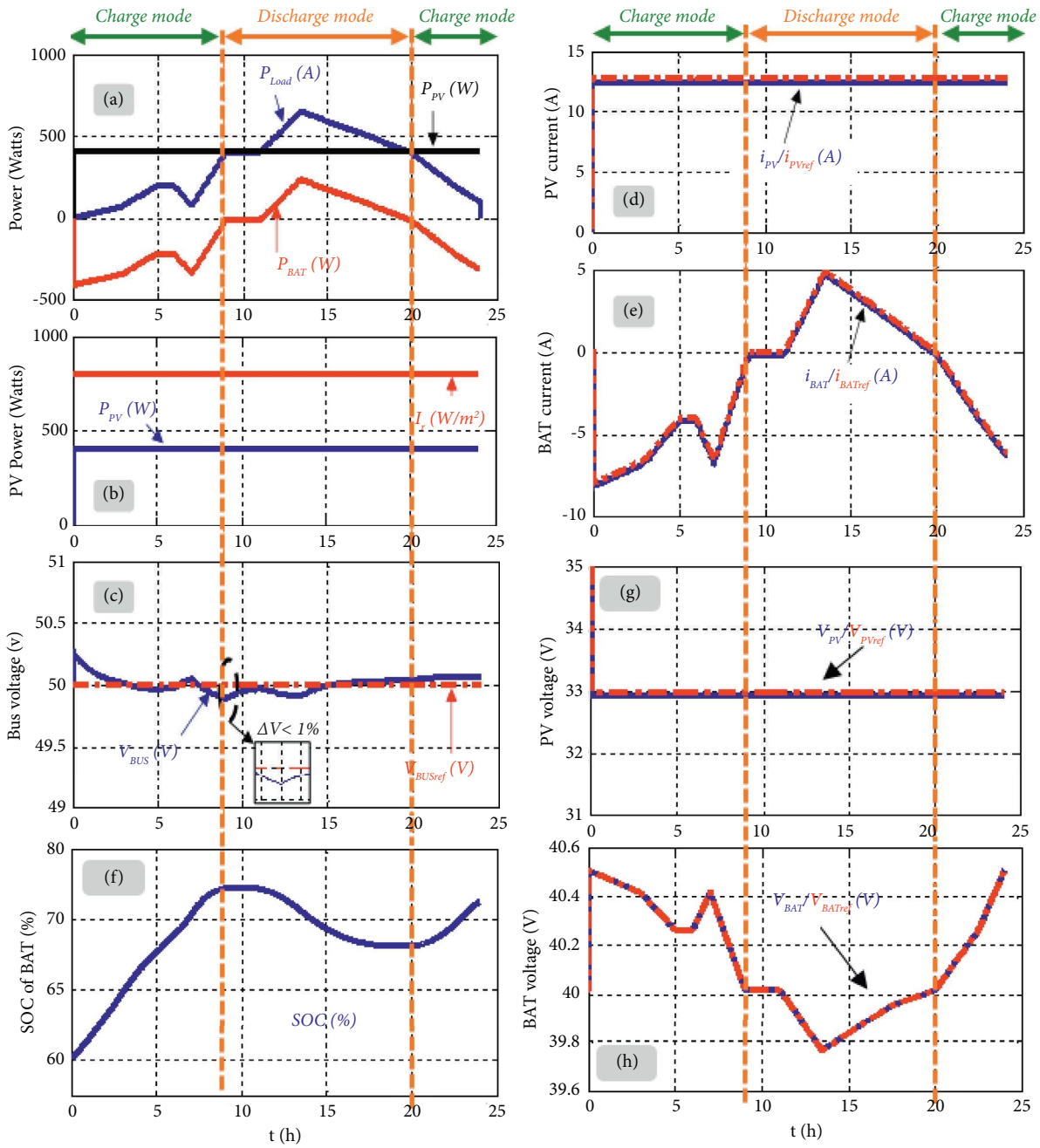

Figure 13: System operation performances under constant solar irradiance.

meeting the load power during the load increase. Reciprocally, the BAT current output switches from the discharge mode to charge mode at 20 h to absorb the DC bus energy when the PV power produced exceeds the required load power. It is worth noting that the negative sign of the BAT current means that the BATs are in the recovery mode (BAT are recovering the energy), and the positive sign of the BAT current implies that the BATs are supplying the load (BATs are in the supply mode).

The regulated DC bus voltage and its reference are shown in Figure 13(c). The common bus voltage is regulated in the desired value and remains at its reference ($V_{\text{Bus\_ref}} = 50$ V); the voltage deviation is very small ($\Delta V < 1\%$). In conclusion, the voltage V_{Bus} fulfills the load demands with high control efficiency. The well-performing V_{Bus} enables correct functioning in the PV-BAT system, where the power balance is achieved.

Figures 13(g) and 13(h) show the controlled voltages and their references on PV and BAT units, respectively. The BAT voltage varies in accordance with the power absorbed/injected into the DC bus. Similar behaviors can be noticed for the PV voltage. The PV and BAT voltages are controlled with a very quick control response, and the largest fluctuations are about 0.2%, conforming to the system design

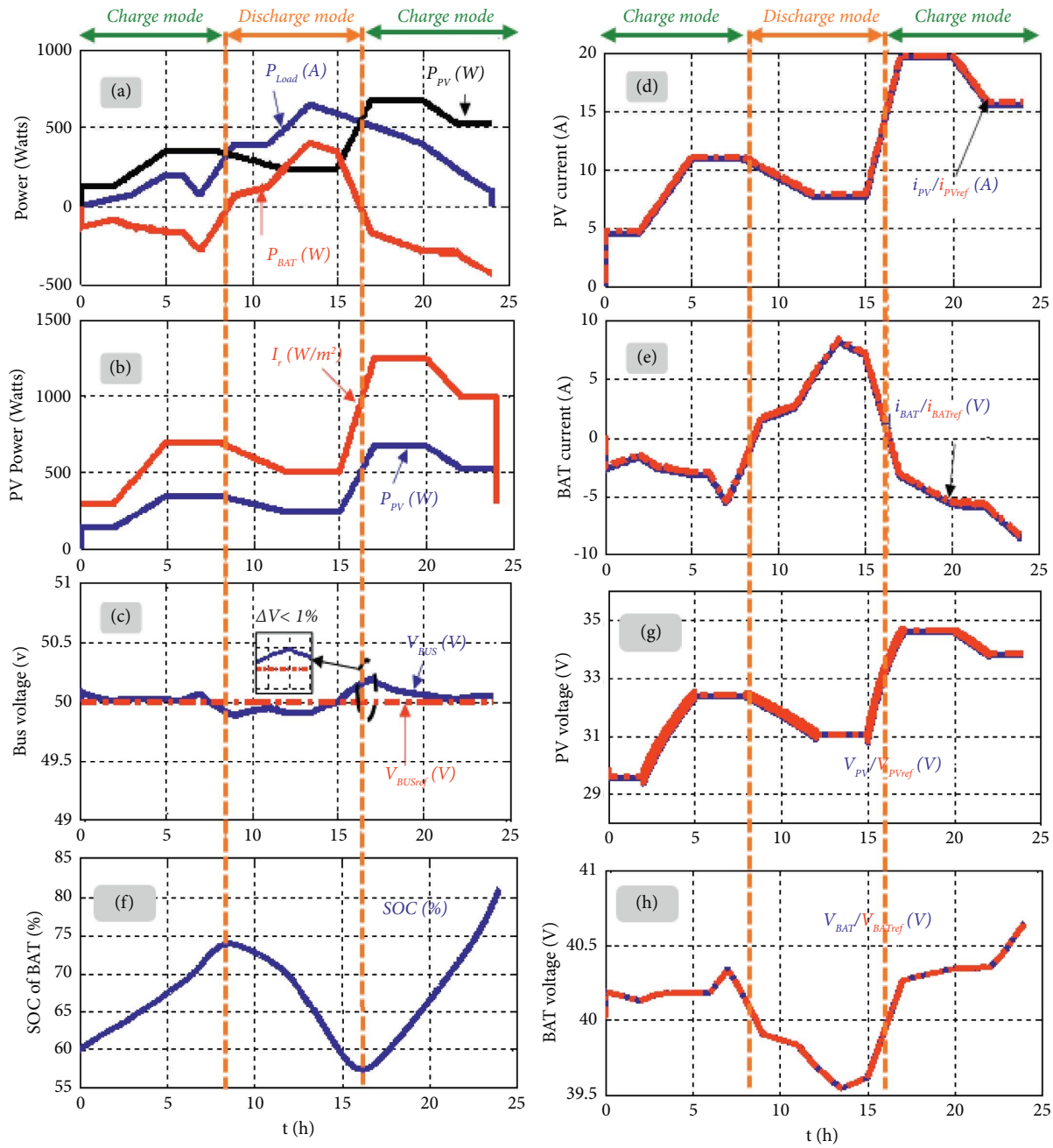

Figure 14: System operation performances under variable solar irradiance.

recommendations. Conclusively, the control achieves the objective of supplying the DC load properly.

5.2. Case 2: Variable Solar Irradiance. These second tests (Figure 14) confirm that the control strategy and the EMS are fully effective in preventing damage while the load attempts to push the system elements to reach or exceed their self-limits.

As BAT approaches the limits of its safety capability, the control strategy changes from normal mode to transient mode, and the EMS continues to maintain power balance by exchanging active power with the load, as shown in Figure 14(a).

When SOC approaches its lower limit at time ranges [15 h 15–16 h 21], the control strategy in BAT is converted into a fuzzy controller according to the explanations of Section 3.2. In Figure 14(a), we can see that the transition is rapid and smooth, and the BAT switching from charge mode to discharge mode at 16 h 21 is also smooth, as shown in Figure 14(e).

The second stage begins once the BAT'SOC approaches its upper limit at a time range [23 h-24 h]. The PV system quits the MPPT operating mode and switches to the fuzzy control (Figure 14(d)) to maintain the DC bus's stabilization.

Table 3: The fluctuation of DC bus.

Time	Fluctuation of DC bus		
	Charge mode (V)	Discharge mode (V)	Charge mode (V)
Figure 13(c)	0.2	0.1	0.1
Figure 14(c)	0.1	0.17	0.2

Table 4: The time balancing of SOC.

Time	Time balancing of SOC		
	Charge mode (sec)	Discharge mode (sec)	Charge mode (sec)
Figure 13(f)	39	41	38
Figure 14(f)	38	49	51

The results in Figure 14(c) show low fluctuation in the DC common bus voltage, which gives the proposed control strategy an advantage.

Controlled voltages on PV and BAT systems and their references are shown in Figures 14(g) and 14(h), respectively. The references are provided to ensure the DC bus voltage regulation; subsequently, the BATs are enabled to stabilize the DC bus voltage through injection or absorption of the erroneous power for balancing the DC bus. The PV voltage varies in accordance with the solar irradiance profile in Figure 14(h). Furthermore, the BAT'SOC is well controlled as, in steady state, BAT voltage is tending towards its reference setting (Figure 14(g)). BATs are temporarily assisting the PV source and involve variations in the BAT voltage. However, the slowness of the PV response guarantees a well-regulated BAT voltage. In fact, this is the explanation for the slight overshooting of the PV power while the BAT voltage is being transiently compensated.

From comparing the results in Figures 13 and 14, we can conclude that the proposed control strategy distributes the load power dynamically effectively between different system units. EMS technique implementation correctly ensures the power sharing between sources (PV and BAT) and load demand. Furthermore, the proposed EMS technique is very efficient in terms of mode changes in accordance with the operating constraints including load fluctuation, PV power generation fluctuation, and BAT quiet operation by using coefficient K_R to adapt the global system's behavior to the operating modes.

It is noted that despite a high current, the DC bus voltage V_{BUS} varies very little (less than 1%) compared to its reference voltage V_{BUSref} set at 50 V. These results clearly indicate the effectiveness of DC bus voltage regulation that contributes to the optimal performance of the suggested EMS. DC bus voltage always follows its reference perfectly (Figures 13(c) and 14(c)), demonstrating the voltage loop effectiveness in DC bus regulation.

Likewise, for current loops, the currents also obey their references for the PV generator (Figures 13(d) and 14(d)) and for the BAT (Figures 13(e) and 14(e)). This shows the significance of the primary control and makes a managed PV-BAT hybrid system capable of increasing the power produced by the complementarity of the PV and BAT sources to meet the power load requirements. The currents follow their references with high efficiency.

In addition, Table 3 demonstrates that the suggested control approach can maintain the deviation of DC bus voltage in a lower range, and Table 4 illustrates that the suggested control algorithm has faster SOC balancing.

By comparing these results with the results of two different approaches given in [46, 49], it can be concluded that the control algorithm and EMS presented throughout the present paper have the most rapid SOC balancing and the smallest DC bus voltage deviations.

6. Conclusion

A new control strategy and EMS for PV-BAT hybrid systems are presented in this paper. The proposed approach combines a smart controller using an adaptive FLC algorithm and novel power management supervision to control the power flow between different energy sources and ensure system efficiency for the stability operation when operating conditions change: load demands, weather conditions, and BAT'SOC.

Specifically, the experimental test results show the following. (1) The MPPT algorithm tracks the PV MPP perfectly, and the MPPT tracking response time is very small (<0.2 s), even under extreme dynamic changing conditions. (2) The closed-loop PI primary controllers track their respective reference values very accurately (dynamic follow-up time <0.2 s), even under extreme dynamic changing conditions. (3) The power management algorithm can very well provide power distribution between the sources and the load. (4) Using controller has provided a great improvement to the overall optimization of the EMS. Compared with the control strategies proposed in the literature, the improved adaptive FLC-based EMS strategy can significantly reduce both the DC bus fluctuation (<2%) and the time balancing of SOC (<51 s), maximize the utilization of the PV source, significantly improve the utilization of the storage system, and maintain the consistency of the BAT SOC.

Abbreviations

RES: Renewable energy source
PV: Photovoltaic
BAT: Battery
MPPT: Maximum power point tracking
PWM: Pulse-width modulation

FLC: Fuzzy logic controller
EMS: Energy management system
BMS: Battery management system

Symbols

P_{pv}: The photovoltaic power (W)
P_{BAT}: The battery power (W)
P_{Load}: The power load demand (W)
$\eta_{PV,}$: PV converter efficiency (%)
η_{BAT}: Battery converter efficiency (%)
η_{Load}: Load converter efficiency (%)
SOC: State of charge (%)
SOC_{max}: Maximum state of charge (%)
SOC_{min}: Minimum state of charge (%)
V_{BUS}: DC bus voltage (V)
$I_{sources}$: The source current (A)
V_{BAT}: Battery voltage (V)
I_{BAT}: Battery current (A)
V_{PV}: PV module voltage (V)
I_{PV}: PV module current (A)
I_{Load}: Load current (A)
V_{BUSref}: DC bus voltage reference (V)
V_{BATref}: Battery voltage reference (V)
I_{BATref}: Battery current reference (A)
V_{PVref}: PV voltage reference (V)
I_{PVref}: PV current reference (A)
V_{BATmax}: Maximum BAT voltage (V)
I_{BATmaw}: Maximum BAT current (A)
I_{BATmin}: Minimum BAT current (A)
V_{PVmax}: Maximum PV voltage (V)
I_{PVmax}: Maximum PV current (A).

Data Availability

No data were used to support this study.

Conflicts of Interest

The authors declare that they have no conflicts of interest.

Acknowledgments

This work was supported by ESTACA'LAB, S2ET Department of the "Ecole Supérieure des Techniques Aéronautiques et de Construction Automobile," ESTACA (Paris, France), and Laboratory of Instrumentation, USTHB, with collaboration of "Centre de Développement des Energies Renouvelables," CDER (Algiers, Algeria). The authors would like to acknowledge the ESTACA'LAB staff for their support in terms of material equipment, data, and technical assistance during the laboratory work.

References

[1] A. Suman, "Role of renewable energy technologies in climate change adaptation and mitigation: a brief review from Nepal," *Renewable and Sustainable Energy Reviews*, vol. 151, Article ID 111524, 2021.

[2] C. Breyer, S. Heinonen, and J. Ruotsalainen, "New consciousness: a societal and energetic vision for rebalancing humankind within the limits of planet Earth," *Technological Forecasting and Social Change*, vol. 114, pp. 7–15, 2017.

[3] IPCC, "IPCC special report on the impacts of global warming of 1.5 °C above pre-industrial levels and related global greenhouse gas emission pathways, in the context of strengthening the global response to the threat of climate change, sustainable development, and efforts to eradicate poverty "Global warming of 1.5°C"," 2018, https://www.ipcc.ch/sr15/.

[4] M. Child and C. Breyer, "Transition and transformation: a review of the concept of change in the progress towards future sustainable energy systems," *Energy Policy*, vol. 107, pp. 11–26, 2017.

[5] C. Breyer, D. Bogdanov, A. Gulagi et al., "On the role of solar photovoltaics in global energy transition scenarios," *Progress in Photovoltaics: Research and Applications*, vol. 25, no. 8, pp. 727–745, 2017.

[6] B. Dursun and E. Aykut, "An investigation on wind/PV/fuel cell/battery hybrid renewable energy system for nursing home in Istanbul," *Proceedings of the Institution of Mechanical Engineers, Part A: Journal of Power and Energy*, vol. 233, no. 5, pp. 616–625, 2019.

[7] IEA, "Renewables 2019. Analysis and forecasts for 2024 international energy agency (IEA)," Market Report Series, International Energy Agency, Paris, France, 2020.

[8] X. Li, D. Hui, and X. Lai, "Battery energy storage station (BESS)-based smoothing control of photovoltaic (PV) and wind power generation fluctuations," *IEEE Transactions on Sustainable Energy*, vol. 4, no. 2, pp. 464–473, 2013.

[9] M. Katsanevakis, R. A. Stewart, and J. Lu, "Aggregated applications and benefits of energy storage systems with application-specific control methods: a review," *Renewable and Sustainable Energy Reviews*, vol. 75, pp. 719–741, 2017.

[10] S. Grillo, M. Marinelli, S. Massucco, and F. Silvestro, "Optimal management strategy of a battery-based storage system to improve renewable energy integration in distribution networks," *IEEE Transactions on Smart Grid*, vol. 3, no. 2, pp. 950–958, 2012.

[11] F. Cebulla, T. Naegler, and M. Pohl, "Electrical energy storage in highly renewable European energy systems: capacity requirements, spatial distribution, and storage dispatch," *Journal of Energy Storage*, vol. 14, pp. 211–223, 2017.

[12] A. Bhattacharjee, H. Samanta, N. Banerjee, and H. Saha, "Development and validation of a real time flow control integrated MPPT charger for solar PV applications of vanadium redox flow battery," *Energy Conversion and Management*, vol. 171, pp. 1449–1462, 2018.

[13] W. Jing, C. H. Lai, D. K. Ling, W. S. H. Wong, and M. D. Wong, "Battery lifetime enhancement via smart hybrid energy storage plug-in module in standalone photovoltaic power system," *Journal of Energy Storage*, vol. 21, pp. 586–598, 2019.

[14] D. Kucevic, B. Tepe, S. Englberger et al., "Standard battery energy storage system profiles: analysis of various applications forstationary energy storage systems using a holistic simulation framework," *Journal of Energy Storage*, vol. 28, Article ID 101077, 2020.

[15] M. Alramlawi, A. Gabash, E. Mohagheghi, and P. Li, "Optimal operation of hybrid PV-battery system considering grid scheduled blackouts and battery lifetime," *Solar Energy*, vol. 161, pp. 125–137, 2018.

[16] P. Singh and J. S. Lather, "Variable structure control for dynamic power-sharing and voltage regulation of DC

microgrid with a hybrid energy storage system," *Int Trans Electr Energ Syst*, vol. 30, no. 9, 2020.

[17] J. Kathiresan, S. K. Natarajan, and G. Jothimani, "Energy management of distributed renewable energy sources for residential DC microgrid applications," *Int Trans Electr Energ Syst*, vol. 30, no. 3, 2020.

[18] S. Kosai, "Dynamic vulnerability in standalone hybrid renewable energy system," *Energy Conversion and Management*, vol. 180, pp. 258–268, 2019.

[19] J. P. Torreglosa, P. García-triviño, L. M. Fernándezramirez, and F. Jurado, "Decentralized energy management strategy based on predictive controllers for a medium voltage direct current photovoltaic electric vehicle charging station," *Energy Conversion and Management*, vol. 108, pp. 1–13, 2016.

[20] G. Angenendt, S. Zurmühlen, H. Axelsen, and D. U. Sauer, "Comparison of different operation strategies for PV battery home storage systems including forecast-based operation strategies," *Applied Energy*, vol. 229, pp. 884–899, 2018.

[21] L. Luo, S. S. Abdulkareem, A. Rezvani et al., "Optimal scheduling of a renewable based microgrid considering photovoltaic system and battery energy storage under uncertainty," *Journal of Energy Storage*, vol. 28, Article ID 101306, 2020.

[22] M. P. Bonkile and V. Ramadesigan, "Power management control strategy using physics-based battery models in standalone PV-battery hybrid systems," *Journal of Energy Storage*, vol. 23, pp. 258–268, 2019.

[23] M. Alowaifeer and A. S. Meliopoulos, "Centralized microgrid energy management system based on successive linearization," in *Proceedings of the North American Power Symposium (NAPS)*, pp. 1–6, Fargo, ND, USA, January 2019.

[24] S. Wang, L. Su, and J. Zhang, "MPI based PSO algorithm for the optimization problem in micro-grid energy management system," in *Proceedings of the Chinese Automation Congress (CAC 2017)*, pp. 4479–4483, Jinan, China, December 2017.

[25] M. G M Abdolrasol, M. A. Hannan, S. M. S. Hussain, T. S. Ustun, M. R. Sarker, and P. J. Ker, "Energy management scheduling for microgrids in the virtual power plant system using artificial neural networks," *Energies*, vol. 14, no. 20, p. 6507, 2021.

[26] M. Shaterabadi and M. A. Jirdehi, "Multi-objective stochastic programming energy management for integrated INVELOX turbines in microgrids: a new type of turbines," *Renewable Energy*, vol. 145, pp. 2754–2769, 2020.

[27] A. Salazar, D. Arcos-Aviles, J. Llanos et al., "Model predictive control-based energy management system for isolated electrothermal microgrids in rural areas of Ecuador," in *Proceedings of the 23rd European Conference on Power Electronics and Applications (EPE'21 ECCE Europe)*, pp. 1–6, Ghent, Belgium, September 2021.

[28] K. A. Al Sumarmad, N. Sulaiman, N. I. A. Wahab, and H. Hizam, "Energy management and voltage control in microgrids using artificial neural networks, PID, and fuzzy logic controllers," *Energies*, vol. 15, no. 1, p. 303, 2022.

[29] M. Sharma, S. Dhundhara, Y. Arya, and S. Prakash, "Frequency stabilization in deregulated energy system using coordinated operation of fuzzy controller and redox flow battery," *International Journal of Energy Research*, vol. 45, no. 5, pp. 7457–7475, 2021.

[30] M. Sharma, S. Dhundhara, Y. Arya, and S. Prakash, "Frequency excursion mitigation strategy using a novel COA optimised fuzzy controller in wind integrated power systems," *IET Renewable Power Generation*, vol. 14, no. 19, pp. 4071–4085, 2020.

[31] Y. Arya and N. Kumar, "Fuzzy gain scheduling controllers for automatic generation control of two-area interconnected electrical power systems," *Electric Power Components and Systems*, vol. 44, no. 7, pp. 737–751, 2016.

[32] D. Arcos-Aviles, J. Pascual, L. Marroyo, P. Sanchis, and F. Guinjoan, "Fuzzy logic-based energy management system design for residential grid-connected microgrids," *IEEE Transactions on Smart Grid*, vol. 9, no. 2, pp. 530–543, Mar. 2018.

[33] F. S. Tidjani, A. Hamadi, A. Chandra, P. Pillay, and A. Ndtoungou, "Optimization of standalone microgrid considering active damping technique and smart power management using fuzzy logic supervisor," *IEEE Transactions on Smart Grid*, vol. 8, no. 1, pp. 475–484, Jan. 2017.

[34] Y. Han, W. Chen, Q. Li, H. Yang, F. Zare, and Y. Zheng, "Two-level energy management strategy for PV-Fuel cell-battery-based DC microgrid," *International Journal of Hydrogen Energy*, vol. 44, no. 35, pp. 19395–19404, 2019.

[35] M. A. Nasr, S. Nikkhah, G. B. Gharehpetian, E. Nasr-Azadani, and S. H. Hosseinian, "A multi-objective voltage stability constrained energy management system for isolated microgrids," *International Journal of Electrical Power & Energy Systems*, vol. 117, Article ID 105646, May 2020.

[36] X. Zhang, L. Liu, Y. Dai, and T. Lu, "Experimental investigation on the online fuzzy energy management of hybrid fuel cell/battery power system for UAVs," *International Journal of Hydrogen Energy*, vol. 43, no. 21, pp. 10094–10103, 2018.

[37] F. J. Vivas, F. Segura, J. M. Andújar et al., "Multi-objective fuzzy logic-based energy management system for microgrids with battery and hydrogen energy storage system," *Electronics*, vol. 9, no. 7, p. 1074, 2020.

[38] M. Zandi, A. Payman, J. Martin, S. Pierfederici, B. Davat, and F. Meibody-Tabar, "Energy management of a fuel cell/supercapacitor/battery power source for electric vehicular applications," *IEEE Transactions on Vehicular Technology*, vol. 60, no. 2, pp. 433–443, 2011.

[39] G. Zhang, W. Chen, and Q. Li, "Modeling, optimization and control of a FC/battery hybrid locomotive based on ADVISOR," *International Journal of Hydrogen Energy*, vol. 42, no. 29, pp. 18568–18583, 2017.

[40] M. A. Balootaki, H. Rahmani, H. Moeinkhah, and A. Mohammadzadeh, "On the Synchronization and Stabilization of fractional-order chaotic systems: recent advances and future perspectives," *Physica A: Statistical Mechanics and Its Applications*, vol. 551, Article ID 124203, 2020.

[41] S. A. G. K. Abadi, T. Khalili, S. I. Habibi, A. Bidram, and J. M. Guerrero, "Adaptive control and management of multiple nano-grids in an islanded dc microgrid system," *IET Generation, Transmission & Distribution*, vol. 17, no. 8, pp. 1799–1815, 2022.

[42] G. R. Chandra Mouli, P. Bauer, and M. Zeman, "Comparison of system architecture and converter topology for a solar powered electric vehicle charging station," in *Proceedings of the 2015 9th International Conference on Power Electronics and ECCE Asia (ICPE-ECCE Asia)*, Seoul, South Korea, June 2015.

[43] N. H. Baharudin, T. M. N. T. Mansur, F. A. Hamid, R. Ali, and M. I. Misrun, "Topologies of DC-DC converter in solar PV applications," *Indonesian Journal of Electrical Engineering and Computer Science*, vol. 8, no. 2, pp. 368–374, 2017.

[44] Y. Zhang, P. E. Campana, A. Lundblad, L. Wang, and J. Yan, "The influence of photovoltaic models and battery models in

system simulation and optimization," *Energy Procedia*, vol. 105, pp. 1184–1191, 2017.

[45] O. Tremblay, L.-A. Dessaint, and A.-I. Dekkiche, "A generic battery model for the dynamic simulation of hybrid electric vehicles," in *Proceedings of the Vehicle Power and Propulsion Conference, VPPC 2007*, pp. 284–289, IEEE, Arlington, TX, USA, September 2007.

[46] P. Bhowmik, S. Chandak, and P. K. Rout, "State of charge and state of power management in a hybrid energy storage system by the self-tuned dynamic exponent and the fuzzy-based dynamic PI controller," *International Transactions on Electrical Energy Systems*, vol. 29, no. 5, 2019.

[47] H. Assem, F. Bouchafa, B. Bouzidi, and A. Hadj Arab, "Fuzzy logic controller in optimizing of power management in standalone photovoltaic system," *Revue des Energies Renouvelables SIENR*, vol. 18, pp. 41–48, 2014.

[48] H. Assem, T. Azib, F. Bouchafaa, A. Hadj Arab, and C. Laarouci, "Limits control and energy saturation management for DC bus regulation in photovoltaic systems with battery storage," *Solar Energy*, vol. 211, pp. 1301–1310, 2020.

[49] H. Ameli, E. Abbasi, M. T. Ameli, and G. Strbac, "A fuzzy-logic-based control methodology for secure operation of a microgrid in interconnected and isolated modes," *International Transactions on Electrical Energy Systems*, vol. 27, no. 11, 2017.